

Generative diffusion models from a PDE perspective

Fei Cao ^{*} Kimball Johnston [†] Thomas Laurent [‡]
Justin Le [†] Sébastien Motsch [†]

January 29, 2025

Contents

1	Introduction	2
2	Reverse diffusion from PDE and SDE perspectives	4
2.1	A PDE approach to reverse diffusion	4
2.1.1	Derivation of the PDE	4
2.1.2	Generalization	6
2.2	An SDE approach to reverse diffusion	6
2.2.1	Forward SDE	6
2.2.2	Reverse SDE	8
3	Reverse diffusion does <i>not</i> generalize	10
3.1	The past of ρ is the future of q	10
3.2	Generated distribution q	11
4	Reverse diffusion in practice	14
4.1	Explicit reverse SDE	14
4.2	Simplified case: ρ_0 Dirac (unique sample)	16
4.3	Score-matching & stable diffusion	18
4.4	Approximative flow and loss function	20
4.5	Overfitting regime and kernel formulation	22
5	Conclusion	24

¹University of Massachusetts Amherst - Department of Mathematics and Statistics, 710 N Pleasant St, Amherst, MA 01003, USA

²Arizona State University - School of Mathematical and Statistical Sciences, 900 S Palm Walk, Tempe, AZ 85287, USA

³Loyola Marymount University, USA

Abstract

Diffusion models have become the de facto framework for generating new datasets. The core of these models lies in the ability to reverse a diffusion process in time. The goal of this manuscript is to explain, from a PDE perspective, how this method works and how to derive the PDE governing the reverse dynamics as well as to study its solution analytically. By linking forward and reverse dynamics, we show that the reverse process’s distribution has its support contained within the original distribution. Consequently, diffusion methods, in their analytical formulation, do not inherently regularize the original distribution, and thus, there is no generalization principle. This raises a question: where does generalization arise, given that in practice it does occur? Moreover, we derive an explicit solution to the reverse process’s SDE under the assumption that the starting point of the forward process is fixed. This provides a new derivation that links two popular approaches to generative diffusion models: stable diffusion (discrete dynamics) and the score-based approach (continuous dynamics). Finally, we explore the case where the original distribution consists of a finite set of data points. In this scenario, the reverse dynamics are explicit (i.e., the loss function has a clear minimizer), and solving the dynamics fails to generate new samples: the dynamics converge to the original samples. In a sense, solving the minimization problem exactly is “*too good for its own good*” (i.e., an overfitting regime).

1 Introduction

In recent years, generative diffusion models such as score-based generative modeling (SGM) and denoising diffusion probabilistic models (DDPM) have witnessed tremendous success in applications including but not limited to image generation [8, 30], text generation [12, 22], audio generation [20, 29], video generation [16], and more [3, 28]. The ever-growing list of relevant literature is vast, and we refer to [4, 5, 9, 15, 24, 32, 35–39] and references therein for a general overview of the diffusion models in machine learning.

In the most elementary scenario, the goal of a generative model is to produce a collection of new samples, denoted by $\{\tilde{\mathbf{x}}_i\}_{i=1}^M$, based solely on a set of available data, denoted by $\{\mathbf{x}_i\}_{i=1}^N$. The aim is for the generated samples to closely resemble the original data while still being distinct¹. Typically, we assume that our available samples $\{\mathbf{x}_i\}_{i=1}^N$ are i.i.d. (independent and identically distributed) and follow an unknown probability distribution $\rho_0 \in \mathcal{P}(\mathbb{R}^d)$ (see figure 1). A popular approach in statistics is to use a kernel density estimation technique to reconstruct an approximation, denoted by q , of ρ_0 from the original sample [31] (see figure 1-A). Afterwards, samples are generated from q . This approach is quite effective in low dimensions but becomes ineffective in high dimensions (e.g., images) since one has to learn the structure of the data first.

¹The Thai expression “*same same, but different*” captures this concept well

To face the curse of dimensionality, a different approach has emerged using (variational) auto-encoders. The idea is to first *encode* or project each sample onto a latent space of lower dimension. This latent space can be interpreted as the key features of the sample. Afterwards, the features are *decoded* in a second step to generate a sample (see figure 1-B). Notice that in this approach, new samples are generated without the need to construct an approximate density q . Diffusion models operate similarly, as they also involve an encoding-decoding process. However, in this case, the encoding phase consists of gradually adding noise to each sample, transforming the (unknown) distribution ρ_0 into a standard Gaussian density \mathcal{N} . Then, a denoising procedure is performed to reconstruct the original data ρ_0 from pure noise by reversing (in time) the forward diffusion process. It is worth noting that the encoding in diffusion models is explicit (in the sense that it requires no training) and does not involve dimensionality reduction. The advantage of this approach is that there is no need to fix a-priori the dimensionality of the latent space. However, the method may be prone to overfitting (e.g., the generated dataset could end up being a mere replication of the training data).

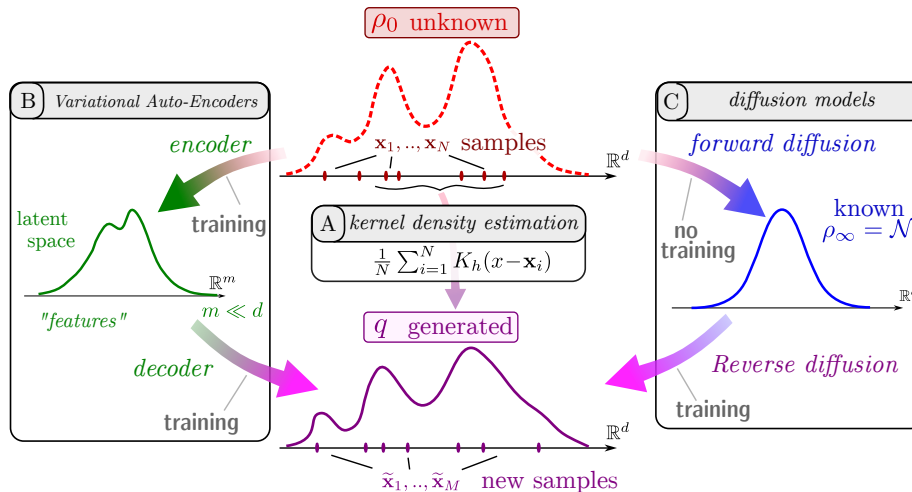


Figure 1: Illustration of various generative models. Given a data sample $\{\mathbf{x}_i\}_{i=1}^N$ from an unknown distribution ρ_0 , the goal is to generate new samples $\{\tilde{\mathbf{x}}_i\}_{i=1}^M$. In kernel density estimation (A), a density q is first estimated, and new samples are then drawn from this estimated distribution. In the auto-encoder approach (B), an encoder-decoder network is trained to reconstruct the samples. Diffusion models (C) work similarly to the auto-encoder method, except only the decoder must be learned, and the encoder does not reduce dimensionality.

Despite the existence of a vast literature on diffusion models and related generative models, a majority of the models require a heavy or advanced background in probability theory and SDEs to explain, design, adjust, and optimize (though some works derive these models from other points of view, including

mean-field-games [41] and optimal transport [6]). One of our main goals in the present manuscript is the re-introduction of the basic diffusion model from a PDE perspective. We believe that this pedestrian’s guide to diffusion models, which highlights their PDE ingredients (and is also suitable for pedagogical purposes), will inspire novel research efforts to investigate the subtle power of such generative models from a PDE viewpoint.

The rest of the manuscript is organized as follows: in section 2.1, we provide a PDE-based approach for the derivation of the reverse diffusion process from the forward diffusion process (i.e., the noising process that turns the data into Gaussian noise). Section 2.2 is devoted to a more traditional derivation of the reversed diffusion process from an SDE perspective. Our derivations in sections 2.1 and 2.2 are sufficiently elementary compared to the technical papers [1, 14]. In section 3, we convey the message that a perfect (reversed) diffusion process will not generalize well. This fact seems to be well-recognized in the machine learning community [21, 33], but we failed to locate a reference offering the precise, mathematical explanation of this phenomenon presented here. The argument presented in section 3 is entirely analytic (as opposed to probabilistic), which reveals the appealing advantage of a PDE approach. We provide a few numerical implementations of the diffusion models in section 4, where the link between score-based generative modeling and stable diffusion is emphasized as well. Lastly, we give our conclusion in section 5 along with a list of important open questions to be addressed in subsequent works.

2 Reverse diffusion from PDE and SDE perspectives

2.1 A PDE approach to reverse diffusion

2.1.1 Derivation of the PDE

We would like to introduce and derive the reverse PDE dynamics used in diffusion models. We will adopt a PDE approach as opposed to the SDE approach frequently encountered in relevant literature [1, 14]. An overview of the problem is given in figure 2. There are two processes at play. First, the forward diffusion process transforms a density distribution ρ_0 into a standard normal distribution \mathcal{N} :

$$\begin{array}{l} \mathbf{Forward} \\ \mathbf{diffusion} \end{array} \quad \begin{cases} \partial_t \rho = \nabla \cdot (x\rho) + \Delta \rho \\ \rho(t=0) = \rho_0. \end{cases} \quad (2.1)$$

This process is known as the Ornstein-Uhlenbeck equation (or the Langevin equation). The law ρ converges exponentially quickly toward the normal distribution under various metrics [2]. In practice, the forward diffusion is only solved up to a finite time T_* , so the resulting distribution $\rho(\cdot, T_*)$ is only exponentially close to the equilibrium distribution \mathcal{N} .

The second step is to *reverse* the dynamics to transform a normal distribution \mathcal{N} back into ρ_0 . A naive way to carry out this step is simply to look at the

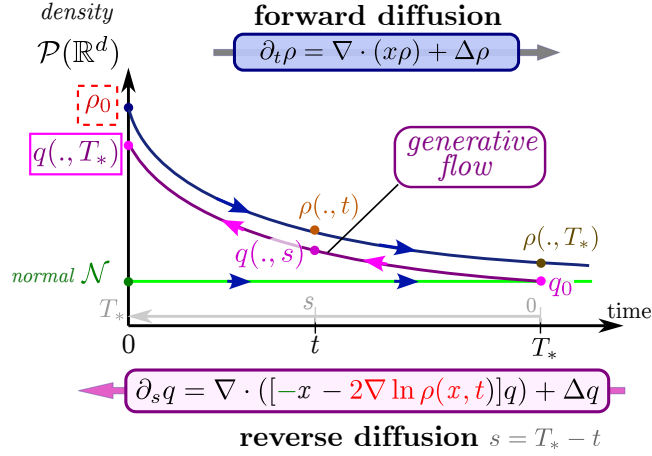


Figure 2: The forward process as a PDE (2.1) transforms any distribution ρ_0 into a normal distribution \mathcal{N} . The reverse process does the opposite and transforms a normal distribution \mathcal{N} into (almost) ρ_0 .

evolution of $\rho(\cdot, t)$ in reverse time by introducing the distribution $q(\cdot, s)$ with

$$q(x, s) := \rho(x, T_* - s) \quad \text{for } 0 \leq s \leq T_*. \quad (2.2)$$

The starting point $s = 0$ corresponds to the final time $t = T_*$. This distribution q satisfies

$$\begin{array}{l} \text{Unstable} \\ \text{Reverse diffusion} \end{array} \quad \begin{cases} \partial_s q = -\nabla \cdot (xq) - \Delta q \\ q(x, s = 0) = \rho(x, T_*) \end{cases} \quad (2.3)$$

This PDE is ill-posed due to the anti-diffusion operator $-\Delta$ (see figure 3). To make the PDE stable while preserving the property (2.2), the key ingredient is to rewrite the diffusion process Δ as a (non-linear) transport equation [7]:

$$\Delta \varphi = \nabla \cdot (\nabla \varphi) = \nabla \cdot (\varphi \nabla \log \varphi). \quad (2.4)$$

We then deduce

$$\Delta \varphi = 2\nabla \cdot (\varphi \nabla \log \varphi) - \Delta \varphi. \quad (2.5)$$

If q satisfies (2.2), we obtain

$$-\Delta q(x, s) = -2\nabla \cdot (q(x, s) \nabla \log \rho(x, T_* - s)) + \Delta q(x, s). \quad (2.6)$$

This motivates the introduction of the reverse diffusion equation for $0 \leq s \leq T_*$:

$$\begin{array}{l} \text{Stable} \\ \text{Reverse diffusion} \end{array} \quad \begin{cases} \partial_s q = \nabla \cdot ([-x - 2\nabla \log \rho(\cdot, T_* - s)] q) + \Delta q \\ q(x, s = 0) = q_0(x) \end{cases} \quad (2.7)$$

In short, we have stabilized the unstable reverse diffusion (2.3) by adding twice the Laplace operator Δ and removing twice the non-linear transport term. In particular, if we take $q_0(x) = \rho(x, T_*)$, then $q(x, s) = \rho(x, T_* - s)$ is the solution to the reverse diffusion (2.7).

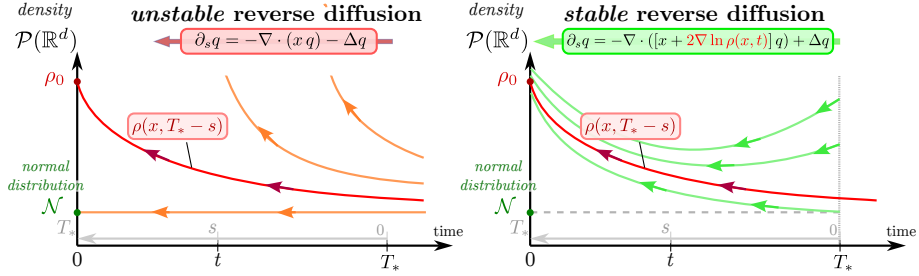


Figure 3: Reversing the forward process (2.1) by reversing time in a naive way (2.2) yields an ill-posed problem (2.3) even though the curve $s \rightarrow \rho(x, T_* - s)$ is a solution. The *true* reverse dynamics (2.7) preserves this curve but also stabilizes the solution. As a consequence, the normal distribution \mathcal{N} is no longer an equilibrium distribution for the (non-autonomous) reverse dynamics.

2.1.2 Generalization

There are other ways to stabilize the unstable reverse diffusion (2.3). For instance, one can add the Laplace operator Δ and remove the non-linear transport term just once each, leading to the following PDE:

$$\partial_s q = \nabla \cdot ([-x - \nabla \log \rho(\cdot, T_* - s)]q). \quad (2.8)$$

As there is no diffusion operator, the associated stochastic process will be deterministic (see further discussions in [18]).

Another generalization is to consider a different forward operator. Instead of using the Ornstein-Uhlenbeck equation (2.1), one can simply use a Brownian motion and its associated generator Δ , leading to the following forward and reverse PDEs:

$$\partial_t \rho = \Delta \rho, \quad (2.9)$$

$$\partial_s q = -\nabla \cdot (2\nabla \log \rho(\cdot, T_* - s)q) + \Delta q. \quad (2.10)$$

Although this formulation simplifies the computations compared with the Ornstein-Uhlenbeck dynamics, there is nonetheless an additional requirement: one needs to introduce a bounded domain with boundary conditions so that the forward dynamics converges to a uniform equilibrium. Without the presence of a boundary, the solution to (2.9) will converge to the zero function [11].

2.2 An SDE approach to reverse diffusion

We now present a more traditional derivation of the reverse dynamics from the SDE perspective. An overview of this approach is encapsulated in figure 4.

2.2.1 Forward SDE

In this subsection, we review the basic properties of the forward diffusion process. Consider a stochastic process X_t in \mathbb{R}^d satisfying the Ornstein-Uhlenbeck

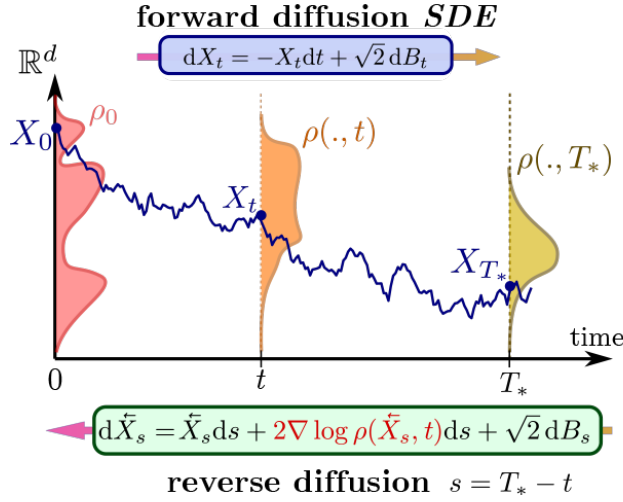


Figure 4: The forward process as an SDE (2.11) transforms the initial law ρ_0 into a standard normal distribution \mathcal{N} , while the reverse process performs the opposite transformation.

dynamics:

$$dX_t = -X_t dt + \sqrt{2} dB_t, \quad (2.11)$$

where B_t is the standard Brownian motion in \mathbb{R}^d . Using an integrating factor, we obtain the explicit solution

$$X_t = e^{-t} X_0 + \sqrt{2} e^{-t} \int_0^t e^z dB_z \sim \mathcal{N}(e^{-t} X_0, \sigma_t^2 \text{Id}), \quad (2.12)$$

where \mathcal{N} is a Gaussian distribution and $\sigma_t^2 := 1 - e^{-2t}$. Thanks to this explicit formula, we can show the convergence of X_t toward the standard normal distribution $\mathcal{N}(\mathbf{0}, \text{Id})$ in various senses [2].

The process X_t naturally induces an operator L (its *generator*) [10, 25]

$$L[\varphi](x) = -x \cdot \nabla \varphi(x) + \Delta \varphi(x). \quad (2.13)$$

In particular, for a given test function φ , if we consider the function

$$u(x, t) = \mathbb{E}[\varphi(X_t) \mid X_0 = x], \quad (2.14)$$

then it follows from Itô's formula that u satisfies the Kolmogorov *backward* equation:

$$\begin{cases} \partial_t u = L[u] \\ u(x, t = 0) = \varphi(x). \end{cases} \quad (2.15)$$

Remark. The terminology *backward* here might be confusing. The Kolmogorov *backward* equation (2.15) follows the process X_t , while the law $\rho(x, t)$

of X_t satisfies the Kolmogorov *forward* equation:

$$\partial_t \rho = L^*[\rho], \quad L^*[\varphi](x) := \nabla \cdot (x \varphi(x)) + \Delta \varphi(x), \quad (2.16)$$

which is precisely (2.1). Both equations evolve *forward* in time.

To conclude our review of the forward process, we consider the process with a terminal condition at a fixed time T_* :

$$v(x, t) = \mathbb{E}[\varphi(X_{T_*}) \mid X_t = x]. \quad (2.17)$$

This satisfies the Feynman-Kac formula [10]:

$$\begin{cases} \partial_t v = -L[v] \\ v(x, t = T_*) = \varphi(x). \end{cases} \quad (2.18)$$

We will need this property to derive the SDE for the reserve process.

2.2.2 Reverse SDE

Now we are ready to derive the reverse diffusion equation (2.7) using stochastic processes. We consider the reverse (in time) trajectories

$$\tilde{X}_s = X_{T_* - s}, \quad (2.19)$$

where X_t is the solution to the forward diffusion (2.11). Our goal is to find the generator associated with the processes \tilde{X}_s . The traditional approach to finding the generator is to consider

$$\tilde{u}(x, s) = \mathbb{E}[\varphi(\tilde{X}_s) \mid \tilde{X}_0 = x] \quad (2.20)$$

and then take the time derivative. However, in this case, it is more convenient to consider the function with a terminal condition:

$$\tilde{v}(x, s) = \mathbb{E}[\varphi(\tilde{X}_{T_*}) \mid \tilde{X}_s = x] \quad (2.21)$$

$$= \mathbb{E}[\varphi(X_0) \mid X_t = x], \quad (2.22)$$

using (2.19) with $t := T_* - s$. Notice that we first have to fix the initial condition ρ_0 for the law of X_0 . To write the function \tilde{v} explicitly, we introduce the joint law of the pairwise process:

$$\rho(x, t_1; y, t_2) = \text{“joint law of } X_{t_1} \text{ and } X_{t_2}\text{”}. \quad (2.23)$$

In particular,

$$\rho(x, 0; y, t) = \rho(y, t \mid x, 0) \cdot \rho_0(x). \quad (2.24)$$

We can now derive the equation satisfied by \tilde{v} .

Proposition 2.1 *The function $\tilde{v}(x, s)$ (2.21) satisfies the following Kolmogorov backward equation:*

$$\begin{cases} \partial_s \tilde{v} = (-x - 2\nabla \log \rho(x, T_* - s)) \cdot \nabla \tilde{v} - \Delta \tilde{v} \\ \tilde{v}(x, s = T_*) = \varphi(x). \end{cases} \quad (2.25)$$

Proof. Let's start by writing \bar{v} using the joint law (2.23):

$$\bar{v}(x, s) = \int_{y \in \mathbb{R}^d} \varphi(y) \rho(y, 0 | x, t) dy \quad (2.26)$$

$$= \int_{y \in \mathbb{R}^d} \varphi(y) \rho(x, t | y, 0) \frac{\rho_0(y)}{\rho(x, t)} dy \quad (2.27)$$

using Bayes' formula. This leads us to

$$\rho(x, t) \bar{v}(x, s) = \int_{y \in \mathbb{R}^d} \varphi(y) \rho(x, t | y, 0) \rho_0(y) dy. \quad (2.28)$$

Taking the derivative with respect to s yields

$$-\partial_t \rho \bar{v} + \rho \partial_s \bar{v} = - \int_{y \in \mathbb{R}^d} \varphi(y) \partial_t \rho(x, t | y, 0) \rho_0(y) dy. \quad (2.29)$$

Using the fact that ρ satisfies the Kolmogorov forward equation (2.16), we obtain

$$-L^*[\rho] \bar{v} + \rho \partial_s \bar{v} = - \int_{y \in \mathbb{R}^d} \varphi(y) L^*[\rho(x, t | y, 0)] \rho_0(y) dy. \quad (2.30)$$

Using the identity (2.28), we arrive at

$$-L^*[\rho] \bar{v} + \rho \partial_s \bar{v} = -L^*[\rho \bar{v}]. \quad (2.31)$$

We then conclude thanks to Lemma 2.2 below. \square

Lemma 2.2 *For any smooth functions p and φ ,*

$$L^*[p\varphi] = L^*[p]\varphi + (xp + 2\nabla p) \cdot \nabla \varphi + p\Delta \varphi. \quad (2.32)$$

Proof. The proof follows from direct computation:

$$L^*[p\varphi] = \nabla \cdot (xp\varphi) + \Delta(p\varphi) \quad (2.33)$$

$$= \nabla \cdot (xp)\varphi + xp \cdot \nabla \varphi + \Delta p \varphi + 2\nabla p \cdot \nabla \varphi + p\Delta \varphi. \quad (2.34)$$

\square

From Proposition 2.1 and the Feynman-Kac formula (2.18), we conclude that the generator of the process \bar{X}_s is a time-dependent operator:

$$R[\varphi(x), s] := (x + 2\nabla \log \rho(x, T_* - s)) \cdot \nabla \varphi(x) + \Delta \varphi(x). \quad (2.35)$$

We then deduce that the law $q(x, s)$ of the process \bar{X}_s satisfies

$$\partial_s q(x, s) = R^*[q(x, s), s], \quad (2.36)$$

with the operator

$$R^*[q(x), s] := \nabla \cdot \left((-x - 2\nabla \log \rho(x, T_* - s)) q(x) \right) + \Delta q(x), \quad (2.37)$$

thus recovering the reverse diffusion equation (2.7).

3 Reverse diffusion does *not* generalize

3.1 The past of ρ is the future of q

Let's consider the forward and reverse dynamics together. Fix two initial distributions ρ_0 and q_0 along with a horizon time T_* , and then consider the forward process X_t with generator L (2.13) and the reverse process \bar{X}_s for $0 \leq s \leq T_*$ with generator R (2.35). Their respective laws $\rho(x, t)$ and $q(x, s)$ are solutions to

$$\begin{cases} \partial_t \rho = L^*[\rho] \\ \rho(x, t = 0) = \rho_0(x) \end{cases} \quad \text{and} \quad \begin{cases} \partial_s q = R^*[q, s] \\ q(x, s = 0) = q_0(x), \end{cases} \quad (3.1)$$

where the operators L^* and R^* are defined by (2.16) and (2.37), respectively.

As we have already introduced the joint law $\rho(\cdot, t_1; \cdot, t_2)$ of the forward process (2.23), we now denote the joint law for the reverse process as

$$q(x, s_1; y, s_2) = \text{“joint law of } \bar{X}_{s_1} \text{ and } \bar{X}_{s_2}\text{”}. \quad (3.2)$$

Remark. Notice that the pairwise distribution $\rho(\cdot; \cdot)$ is time-homogeneous while $q(\cdot; \cdot)$ is not. In other words, we have the property that for $t_1 < t_2$ and any t_0 ,

$$\rho(y, t_2 \mid x, t_1) = \rho(y, t_2 + t_0 \mid x, t_1 + t_0). \quad (3.3)$$

This is not the case for $q(\cdot \mid \cdot)$, which reflects the time dependency of its generator R (2.35).

We can link the two joint laws (2.23) and (3.2): backtracking into the past of ρ is equivalent to looking into the future of q (see the illustration in figure 5).

Theorem 1 *For any $0 \leq t_1 < t_2 \leq T_*$ and any $x, y \in \mathbb{R}^d$, we have*

$$\rho(x, t_1 \mid y, t_2) = q(x, s_1 \mid y, s_2), \quad (3.4)$$

with $s_1 = T_* - t_1$ and $s_2 = T_* - t_2$.

Proof. Fix $y \in \mathbb{R}^d$ and $t_1 \in [0, T_*]$, and take a test function φ . Consider s and t such that $t_1 \leq t = T_* - s \leq T_*$, meaning $0 \leq s \leq T_* - t_1 = s_1$. Define the function

$$a(y, s) = \int_{x \in \mathbb{R}^d} \varphi(x) \rho(x, t_1 \mid y, T_* - s) dx \quad (3.5)$$

$$= \mathbb{E}[\varphi(X_{t_1}) \mid X_{T_* - s} = y] \quad (3.6)$$

$$= \mathbb{E}[\varphi(X_{t_1}) \mid X_t = y]. \quad (3.7)$$

Following the same strategy as in the proof of Proposition 2.1, we find that

$$\partial_s a(y, s) = -R[a(y, s), s]. \quad (3.8)$$

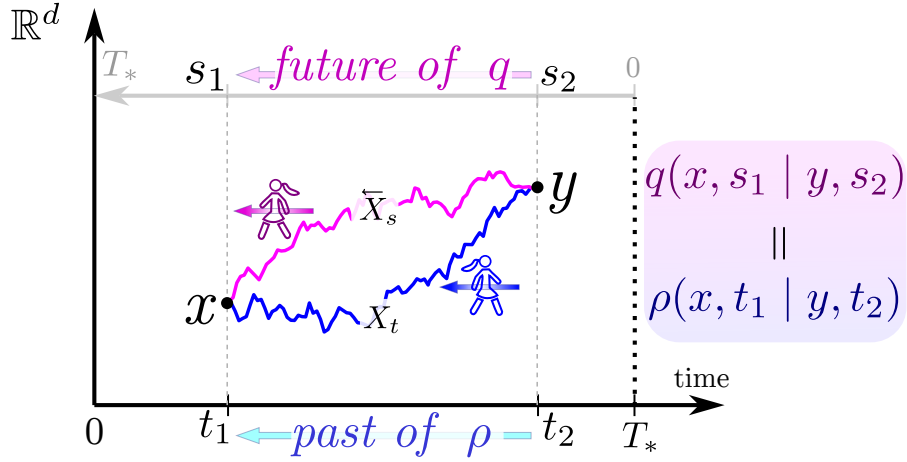


Figure 5: Illustration of Theorem 1 and the identity (3.4). The (density of the) probability that $X_{t_1} = x$ (past) knowing that $X_{t_2} = y$ (future) is the same as the probability that $\tilde{X}_{s_1} = x$ (future) knowing that $\tilde{X}_{s_2} = y$ (past).

Thus, we have that a satisfies

$$\begin{cases} \partial_s a(y, s) = -R[a(y, s), s] \\ a(y, s = T_* - t_1 = s_1) = \varphi(y), \end{cases} \quad (3.9)$$

where $0 \leq s \leq s_1$.

Now, an application of the Feynman-Kac formula (see for instance Proposition 3.41 in [26]) yields

$$a(y, s) = \mathbb{E}[\varphi(Y_{s_1}) | Y_s = y], \quad (3.10)$$

where (Y_s) is a Markov process with generator R . On the other hand, we have already seen that (\tilde{X}_s) is exactly such a process. Hence, we conclude

$$a(y, s) = \mathbb{E}[\varphi(\tilde{X}_{s_1}) | \tilde{X}_s = y]. \quad (3.11)$$

Finally, using the definition of a , we deduce that

$$\mathbb{E}[\varphi(X_{t_1}) | X_t = y] = \mathbb{E}[\varphi(\tilde{X}_{s_1}) | \tilde{X}_s = y], \quad (3.12)$$

where $t_1 = T_* - s_1$ and $t = T_* - s$.

If we set $t_2 = t$ and $s_2 = s = T_* - t_2$, then since the equation (3.12) is satisfied for any test function φ , we arrive at the advertised identity (3.4). \square

3.2 Generated distribution q

Thanks to Theorem 1, we deduce the behavior of the reverse process \tilde{X}_s as s approaches T_* (i.e., when $t \rightarrow 0$).

Corollary 3.1 For any $x, y \in \mathbb{R}^d$, the pairwise distributions of ρ (2.23) and q (3.2) satisfy

$$q(y, T_* | x, 0) = \rho_0(y) \cdot \frac{\rho(x, T_* | y, 0)}{\rho(x, T_*)}. \quad (3.13)$$

Proof. Let's again consider the function \tilde{u} (2.20) with a test function φ :

$$\tilde{u}(x, s) = \mathbb{E}[\varphi(\tilde{X}_s) | \tilde{X}_0 = x] = \int_{y \in \mathbb{R}^d} \varphi(y) q(y, s | x, 0) dy \quad (3.14)$$

$$= \int_{y \in \mathbb{R}^d} \varphi(y) \rho(y, t | x, T_*) dy \quad (3.15)$$

$$= \int_{y \in \mathbb{R}^d} \varphi(y) \rho(x, T_* | y, t) \frac{\rho(y, t)}{\rho(x, T_*)} dy \quad (3.16)$$

$$\xrightarrow{s \rightarrow T_*} \int_{y \in \mathbb{R}^d} \varphi(y) \rho(x, T_* | y, 0) \frac{\rho_0(y)}{\rho(x, T_*)} dy. \quad (3.17)$$

This completes the proof of (3.13). \square

As the law $\rho(x, T_* | y, 0)$ is entirely explicit, i.e., $\rho(\cdot, T_* | y, 0) \sim \mathcal{N}(e^{-T_*} y, \sigma_{T_*}^2 \text{Id})$ with $\sigma_{T_*}^2 = 1 - e^{-2T_*}$, we can even write an explicit formula:

$$q(y, T_* | x, 0) = \rho_0(y) \frac{\exp\left(-\frac{|ye^{-T_*} - x|^2}{2\sigma_{T_*}^2}\right)}{\int_{z \in \mathbb{R}^d} \rho_0(z) \exp\left(-\frac{|ze^{-T_*} - x|^2}{2\sigma_{T_*}^2}\right) dz}. \quad (3.18)$$

Corollary 3.2 The law of \tilde{X}_s at the final time $s = T_*$ is given by

$$q(y, T_*) = \rho_0(y) \int_{x \in \mathbb{R}^d} \rho(x, T_* | y, 0) \frac{q_0(x)}{\rho(x, T_*)} dx. \quad (3.19)$$

Proof. We simply notice that

$$q(y, T_*) = \int_{x \in \mathbb{R}^d} q(y, T_* | x, 0) q_0(x) dx \quad (3.20)$$

and then combine it with (3.13). \square

We notice that if we choose $q_0(x) = \rho(x, T_*)$, then we recover the initial distribution for the forward process, in the sense that $q(y, T_*) = \rho_0(y)$.

Remark. As an immediate by-product of Corollary 3.2, we deduce the pointwise convergence of $q(y, T_*)$ to $\rho_0(y)$ as $T_* \rightarrow +\infty$ (at least for smooth ρ_0). Other works have investigated bounds on the distance between $q(\cdot, T_*)$ and ρ_0 under various hypothesis in a variety of senses, such as KL divergence [34], total variation [6], and types of integral probability metrics [23].

On the other hand, the main consequence of Corollary 3.2 is the realization that the *exact* reverse diffusion does *not* generalize (see the illustration in figure 6).

4 Reverse diffusion in practice

4.1 Explicit reverse SDE

We would like to provide a more practical expression of the reverse dynamics. Recall that the process \tilde{X}_s has its generator R given by (2.35). Consequently, we conclude that \tilde{X}_s is driven by the following Itô diffusion:

$$d\tilde{X}_s = \tilde{X}_s ds + 2 \nabla \ln \rho \left(\tilde{X}_s, T_* - s \right) ds + \sqrt{2} dB_s, \quad (4.1)$$

where $\nabla \ln \rho$ is known as the *score* [35] of the distribution ρ . To get a more explicit expression of the score $\nabla \ln \rho$, we consider the law of X_0 conditioned on $X_t = x$ and denote the expected value

$$\bar{x}_0(x, t) = \mathbb{E}[X_0 | X_t = x]. \quad (4.2)$$

In analogy with the method of characteristics encountered in the study of transport-type PDEs, \bar{x}_0 represents the average “foot” of the characteristics passing through x at time t (see figure 7 for an illustration). Using the pairwise distribution $\rho(\cdot | \cdot)$ (2.23), we can express \bar{x}_0 explicitly and deduce an expression for the score.

Lemma 4.1 *If $X_0 \sim \rho_0$, we can recast \bar{x}_0 as*

$$\bar{x}_0(x, t) = \frac{\int_{y \in \mathbb{R}^d} y \rho(x, t | y, 0) \rho_0(y) dy}{\rho(x, t)}, \quad (4.3)$$

and the score $\nabla \ln \rho$ as:

$$\nabla \ln \rho(x, t) = \frac{e^{-t} \bar{x}_0(x, t) - x}{1 - e^{-2t}}. \quad (4.4)$$

Proof. By Bayes’ rule, we have

$$\rho(y, 0 | x, t) = \frac{\rho(x, t | y, 0) \rho_0(y)}{\rho(x, t)}.$$

We then apply this equality in the definition of \bar{x}_0 :

$$\bar{x}_0(x, t) = \mathbb{E}[X_0 | X_t = x] = \int_{y \in \mathbb{R}^d} y \rho(y, 0 | x, t) dy = \frac{\int_{y \in \mathbb{R}^d} y \rho(x, t | y, 0) \rho_0(y) dy}{\rho(x, t)}.$$

Since $\rho(x, t | y, 0)$ is an explicit Gaussian density, we deduce:

$$\nabla_x \rho(x, t | y, 0) = \rho(x, t | y, 0) \cdot \left(-\frac{x - \alpha_t y}{\beta_t} \right) \quad (4.5)$$

with $\alpha_t = e^{-t}$ and $\beta_t = 1 - e^{-2t}$. Therefore we can rewrite the score $\nabla \ln \rho$ as follows:

$$\begin{aligned} \nabla \ln \rho(x, t) &= \frac{\nabla \rho(x, t)}{\rho(x, t)} = \frac{\int_{y \in \mathbb{R}^d} \nabla_x \rho(x, t | y, 0) \rho_0(y) dy}{\rho(x, t)} \\ &= \frac{\int_{y \in \mathbb{R}^d} \rho(x, t | y, 0) \left(-\frac{x - \alpha_t y}{\beta_t} \right) \rho_0(y) dy}{\rho(x, t)} \\ &= \frac{-\frac{x}{\beta_t} \int_{y \in \mathbb{R}^d} \rho(x, t | y, 0) \rho_0(y) dy + \frac{\alpha_t}{\beta_t} \int_{y \in \mathbb{R}^d} y \rho(x, t | y, 0) \rho_0(y) dy}{\rho(x, t)} \\ &= -\frac{x}{\beta_t} + \frac{\alpha_t}{\beta_t} \bar{\mathbf{x}}_0(x, t). \end{aligned}$$

□

Thanks to the previous lemma, we can express the reverse diffusion process in terms of $\bar{\mathbf{x}}_0$.

Proposition 4.2 *The reverse diffusion dynamics (4.1) can be rewritten as*

$$d\bar{X}_s = \bar{X}_s ds + 2 \frac{\alpha_t \bar{\mathbf{x}}_0(\bar{X}_s, t) - \bar{X}_s}{\beta_t} ds + \sqrt{2} dB_s, \quad (4.6)$$

with $t = T_* - s$, $\alpha_t = e^{-t}$, $\beta_t = 1 - e^{-2t}$ and $\bar{\mathbf{x}}_0$ given by (4.2).

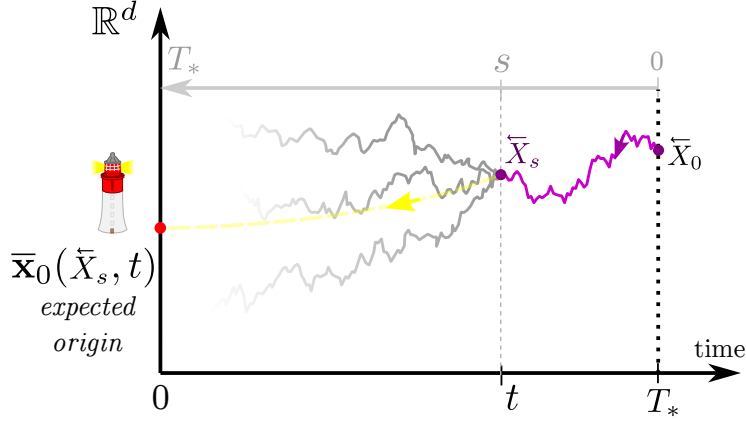


Figure 7: Solving the reverse diffusion written as a SDE (4.6) requires computing $\bar{\mathbf{x}}_0$ (4.2), the expected “foot” of the characteristics passing through point x at time t . This information, like a lighthouse, guides the process \bar{X}_s back to ρ_0 .

Remark. When $t \gg 1$ is large, the reverse diffusion reduces to the forward diffusion process (2.11):

$$d\bar{X}_s \stackrel{t \gg 1}{\approx} \bar{X}_s ds + 2 \frac{\mathbf{0} - \bar{X}_s}{1} ds + \sqrt{2} dB_s = -\bar{X}_s ds + \sqrt{2} dB_s. \quad (4.7)$$

However, when $t \approx 0$, the reverse diffusion becomes a stiff relaxation towards $\bar{\mathbf{x}}_0$:

$$d\tilde{X}_s \stackrel{t \approx 0}{\approx} \frac{1}{t} (\bar{\mathbf{x}}_0 - \tilde{X}_s) ds + \mathcal{O}(1) ds + \sqrt{2} dB_s, \quad (4.8)$$

with $\bar{\mathbf{x}}_0 = \bar{\mathbf{x}}_0(\tilde{X}_s, T_* - s)$ and $t = T_* - s$. If we neglect the $\mathcal{O}(1)$ term and assume that $\bar{\mathbf{x}}_0$ is constant, then this SDE can be explicitly solved by applying the Itô's formula to $\tilde{X}_s/(T_* - s)$:

$$d\tilde{X}_s = \frac{1}{t} (\bar{\mathbf{x}}_0 - \tilde{X}_s) ds + \sqrt{2} dB_s \Rightarrow \tilde{X}_s = \tilde{X}_0 + \frac{t}{T_*} (\bar{\mathbf{x}}_0 - \tilde{X}_0) + Z_s \quad (4.9)$$

where $Z_s = \sqrt{2} t \int_{r=0}^s \frac{dB_r}{T_* - r}$ is a centered Gaussian distribution with covariance matrix $(2t s/T_*) \cdot \text{Id}$. Under these simplifications, the process \tilde{X}_s converges linearly to $\bar{\mathbf{x}}_0$ as $s \rightarrow T_*$ (i.e., $t \rightarrow 0$). It is similar to a Brownian bridge interpolating \tilde{X}_0 and $\bar{\mathbf{x}}_0$ on the interval $s \in [0, T_*]$.

Remark. We can also rewrite the reverse diffusion process in ways that involve hyperbolic trigonometric functions. For instance, we have

$$d\tilde{X}_s = \frac{1}{\tanh(T_* - s)} \left(\frac{\bar{\mathbf{x}}_0(\tilde{X}_s, T_* - s)}{\cosh(T_* - s)} - \tilde{X}_s \right) ds + \sqrt{2} dB_s. \quad (4.10)$$

Using the identity $\tanh(x/2) = \frac{\cosh(x)-1}{\sinh(x)}$ and the definition $\text{csch}(x) = \frac{1}{\sinh(x)}$, equation (4.10) can also be rewritten as

$$d\tilde{X}_s = -\tanh\left(\frac{T_* - s}{2}\right) \tilde{X}_s ds + \text{csch}(T_* - s) (\bar{\mathbf{x}}_0(\tilde{X}_s, T_* - s) - \tilde{X}_s) ds + \sqrt{2} dB_s. \quad (4.11)$$

4.2 Simplified case: ρ_0 Dirac (unique sample)

The explicit reverse dynamics (4.6) is in general nonlinear and therefore not explicitly solvable. However, if we suppose that all the forward trajectories X_t originate from the same origin x_0 (i.e., $\rho_0 = \delta_{x_0}$), then $\bar{\mathbf{x}}_0$ (4.2) is constant and independent of \tilde{X}_s . We can solve the reverse dynamics explicitly in this case, which will be useful in designing a numerical scheme afterwards.

Theorem 2 *If $X_0 = x_0$ is fixed (i.e., if $\rho_0 = \delta_{x_0}$ for some $x_0 \in \mathbb{R}^d$), then*

$$\tilde{X}_s = \frac{\sinh(T_* - s)}{\sinh(T_*)} \tilde{X}_0 + \frac{\sinh(s)}{\sinh(T_*)} x_0 + \sqrt{2 \sinh(T_* - s) \frac{\sinh(s)}{\sinh(T_*)}} \epsilon, \quad (4.12)$$

where $\epsilon \sim \mathcal{N}(\mathbf{0}, \text{Id})$ is a standard Gaussian random vector in dimension d .

Proof. The proof is based on the search for a suitable integrating factor. To begin with, we define $u(s) = -\ln\left(\frac{\sinh(T_*-s)}{\sinh(T_*)}\right)$ and thus $e^{u(s)} = \frac{\text{csch}(T_*-s)}{\text{csch}(T_*)}$. Multiplying both sides of the SDE (4.11) by $e^{u(s)}$ and rearranging the resulting equation, we obtain

$$\begin{aligned} e^{u(s)} d\tilde{X}_s + e^{u(s)} \left(\tanh\left(\frac{T_*-s}{2}\right) + \text{csch}(T_*-s) \right) \tilde{X}_s ds \\ = e^{u(s)} \text{csch}(T_*-s) \bar{x}_0 \left(\tilde{X}_s, T_*-s \right) ds + e^{u(s)} \sqrt{2} dB_s. \end{aligned}$$

Since

$$\frac{d}{ds} \left(e^{u(s)} \right) = e^{u(s)} \left(\tanh\left(\frac{T_*-s}{2}\right) + \text{csch}(T_*-s) \right),$$

we have

$$d \left(e^{u(s)} \tilde{X}_s \right) = e^{u(s)} \text{csch}(T_*-s) \bar{x}_0 \left(\tilde{X}_s, T_*-s \right) ds + e^{u(s)} \sqrt{2} dB_s.$$

Thus

$$e^{u(s)} \tilde{X}_s = e^{u(0)} \tilde{X}_0 + \int_0^s e^{u(r)} \text{csch}(T_*-r) \bar{x}_0 \left(\tilde{X}_r, T_*-r \right) dr + \int_0^s e^{u(r)} \sqrt{2} dB_r. \quad (4.13)$$

As $X_0 = x_0$ is fixed by our assumption, $\bar{x}_0 \left(\tilde{X}_r, T_*-r \right) = x_0$, and

$$\begin{aligned} \int_0^s e^{u(r)} \text{csch}(T_*-r) \bar{x}_0 \left(\tilde{X}_r, T_*-r \right) dr &= \int_0^s \frac{\text{csch}^2(T_*-r)}{\text{csch}(T_*)} x_0 dr \\ &= \frac{\coth(T_*-s) - \coth(T_*)}{\text{csch}(T_*)} x_0. \end{aligned} \quad (4.14)$$

Inserting (4.14) into (4.13) and rearranging, we find

$$\begin{aligned} \tilde{X}_s &= e^{-u(s)} e^{u(0)} \tilde{X}_0 + e^{-u(s)} \frac{\coth(T_*-s) - \coth(T_*)}{\text{csch}(T_*)} x_0 + e^{-u(s)} \int_0^s e^{u(r)} \sqrt{2} dB_r \\ &= \frac{\sinh(T_*-s)}{\sinh(T_*)} \tilde{X}_0 + \left(\frac{\sinh(T_*-s)}{\sinh(T_*)} \right) \left(\frac{\coth(T_*-s) - \coth(T_*)}{\text{csch}(T_*)} \right) x_0 \\ &\quad + \frac{\sinh(T_*-s)}{\sinh(T_*)} \int_0^s e^{u(r)} \sqrt{2} dB_r \\ &= \frac{\sinh(T_*-s)}{\sinh(T_*)} \tilde{X}_0 + \sinh(T_*-s) (\coth(T_*-s) - \coth(T_*)) x_0 \\ &\quad + \frac{\sinh(T_*-s)}{\sinh(T_*)} \int_0^s e^{u(r)} \sqrt{2} dB_r. \end{aligned} \quad (4.15)$$

Notice that $\sinh(T_*-s) (\coth(T_*-s) - \coth(T_*)) = \frac{\sinh(s)}{\sinh(T_*)}$, from which we arrive at the following simplified expression for the variance of (each independent

component of) the Itô integral in (4.15):

$$\begin{aligned}
\frac{\sinh^2(T_* - s)}{\sinh^2(T_*)} \int_0^s 2 e^{2u(r)} dr &= 2 \frac{\sinh^2(T_* - s)}{\sinh^2(T_*)} \int_0^s \frac{\operatorname{csch}^2(T_* - s)}{\operatorname{csch}^2(T_*)} dr \\
&= 2 \left(\frac{\sinh^2(T_* - s)}{\sinh^2(T_*)} \right) \left(\frac{\coth(T_* - s) - \coth(T_*)}{\operatorname{csch}^2(T_*)} \right) \\
&= 2 \sinh(T_* - s) \frac{\sinh(s)}{\sinh(T_*)}.
\end{aligned} \tag{4.16}$$

As \tilde{X}_s is a d -dimensional Gaussian random vector with independent components (due to the non-randomness of \bar{x}_0), we obtain (4.12). \square

As an immediate corollary from Theorem 2, we deduce that the law $q(\cdot, s)$ of \tilde{X}_s converges in Wasserstein distance toward the initial distribution $\rho_0 = \delta_{x_0}$:

$$W_2(q(\cdot, s), \rho_0) = W_2(q(\cdot, s), \delta_{x_0}) \xrightarrow{s \rightarrow T} 0 \tag{4.17}$$

for any $q_0 = q(\cdot, 0) \in \mathcal{P}(\mathbb{R}^d)$ with a finite second moment, where $W_2(\cdot, \cdot)$ represents the usual Wasserstein distance of order 2 between probability measures on \mathbb{R}^d . Indeed, it suffices to show (4.17) in one space dimension (i.e., when $d = 1$) thanks to the independence of components of the d -dimensional Gaussian \tilde{X}_s . By our explicit formula (4.12) for \tilde{X}_s , we readily see that $\mathbb{E}[\tilde{X}_s] \xrightarrow{s \rightarrow T} x_0$ and $\operatorname{Var}[\tilde{X}_s] \xrightarrow{s \rightarrow T} 0$, whence

$$W_2^2(q(\cdot, s), \delta_{x_0}) \leq \mathbb{E}[|\tilde{X}_s - x_0|^2] = \mathbb{E}[(\tilde{X}_s)^2] - 2\mathbb{E}[\tilde{X}_s]x_0 + x_0^2 \xrightarrow{s \rightarrow T} 0. \tag{4.18}$$

4.3 Score-matching & stable diffusion

From the SDE (4.6), we would like to derive a numerical scheme to update \tilde{X}_s at discrete times. The main challenge is to estimate \bar{x}_0 (4.3) since ρ_0 is unknown (we only have access to the sample $\{\mathbf{x}_i\}_{i=1}^N$). We will discuss this task in the following subsection. Let's focus here on the numerical scheme assuming that we can compute \bar{x}_0 in *some way*.

Let's denote a partition $0 = s_0 < s_1 < \dots < s_{n_*} = T_*$ with $\Delta s_n = s_{n+1} - s_n$. The goal is to find a recursive formula to express $\tilde{X}_{s_{n+1}}$ as a function of \tilde{X}_{s_n} . A simple but somewhat naive method consists in applying the Euler-Maruyama method [19] to the reverse SDE (4.6):

$$\begin{aligned}
&\textbf{Euler} \\
&\textbf{Maruyama} : \quad \tilde{X}_{s_{n+1}} = \tilde{X}_{s_n} + \Delta s_n \cdot \left(\tilde{X}_{s_n} + 2 \frac{\alpha_{t_n} \bar{x}_0(\tilde{X}_{s_n}, t_n) - \tilde{X}_{s_n}}{\beta_{t_n}} \right) + \sqrt{\Delta s_n} \epsilon_n
\end{aligned} \tag{4.19}$$

with $t_n = T_* - s_n$, $\alpha_{t_n} = e^{-t_n}$, $\beta_{t_n} = 1 - e^{-2t_n}$ and $\epsilon_n \sim \mathcal{N}(\mathbf{0}, \operatorname{Id})$.

The Euler-Maruyama scheme assumes that the right hand side of the SDE (4.6) is frozen over the time interval $[s_n, s_{n+1}]$. A more subtle method is to assume only \bar{x}_0 is constant over the time interval $[s_n, s_{n+1}]$. Denoting this

constant value by $\langle \bar{\mathbf{x}}_0 \rangle$, we can simplify the nonlinear SDE (4.6) into a linear SDE as in (4.11):

$$d\tilde{X}_s = -\tanh\left(\frac{t}{2}\right) \tilde{X}_s ds + \operatorname{csch}(t) \left(\langle \bar{\mathbf{x}}_0 \rangle - \tilde{X}_s \right) ds + \sqrt{2} dB_s. \quad (4.20)$$

Then we can apply the same strategy as in Theorem 2 to integrate exactly over the time interval $[s_n, s_{n+1}]$ via integrating factor:

$$\begin{aligned} \tilde{X}_{s_{n+1}} &= \frac{\sinh(t_{n+1})}{\sinh(t_n)} \tilde{X}_{s_n} + \frac{\sinh(\Delta s_n)}{\sinh(t_n)} \langle \bar{\mathbf{x}}_0 \rangle \\ \text{Stable Diffusion :} &+ \sqrt{2 \sinh(t_{n+1}) \frac{\sinh(\Delta s_n)}{\sinh(t_n)}} \epsilon_n, \end{aligned} \quad (4.21)$$

with $t_n = T_* - s_n$ (notice $t_{n+1} < t_n$). We emphasize that the formula (4.21) is exact only because we have assumed that $\bar{\mathbf{x}}_0$ is constant over the time interval $[s_n, s_{n+1}]$.

The recursive formula (4.21) appears quite convoluted, but it corresponds exactly to the formula used in the stable diffusion [15]. Indeed, the derivation of the recursive formula for \tilde{X}_s is also exact when we assume $\bar{\mathbf{x}}_0$ is given.

Proposition 4.3 *The recursive formula (4.21) is equivalent to*

$$\tilde{X}_{s_{n+1}} = \mu_{n+1} + \sigma_{n+1} \epsilon_n, \quad (4.22)$$

with $\epsilon_n \sim \mathcal{N}(\mathbf{0}, Id)$ a standard Gaussian and

$$\mu_{n+1} = \frac{e^{-\Delta s_n} (1 - e^{-2t_{n+1}})}{1 - e^{-2t_n}} \tilde{X}_{s_n} + \frac{e^{-t_{n+1}} (1 - e^{-2\Delta s_n})}{1 - e^{-2t_n}} \langle \bar{\mathbf{x}}_0 \rangle, \quad (4.23)$$

$$\sigma_{n+1}^2 = \frac{(1 - e^{-2t_{n+1}})(1 - e^{-2\Delta s_n})}{1 - e^{-2t_n}}. \quad (4.24)$$

One can replace Δs_n by $|\Delta t_n|$ since $|\Delta t_n| = |t_{n+1} - t_n| = |-s_{n+1} + s_n| = \Delta s_n$.

Proof. Without loss of generality and for the sake of notational simplicity, we work with $d = 1$. Let us start from the formula (4.21):

$$\begin{aligned} \mathbb{E}[\tilde{X}_{s_{n+1}} | \tilde{X}_{s_n}] &= \frac{\sinh(t_{n+1})}{\sinh(t_n)} \tilde{X}_{s_n} + \frac{\sinh(\Delta s_n)}{\sinh(t_n)} \langle \bar{\mathbf{x}}_0 \rangle \\ &= \frac{e^{t_n - \Delta s_n} - e^{-t_n + \Delta s_n}}{e^{t_n} - e^{-t_n}} \tilde{X}_{s_n} + \frac{e^{\Delta s_n} - e^{-\Delta s_n}}{e^{t_n} - e^{-t_n}} \langle \bar{\mathbf{x}}_0 \rangle \\ &= \frac{e^{-\Delta s_n} (1 - e^{-2t_n + 2\Delta s_n})}{1 - e^{-2t_n}} \tilde{X}_{s_n} + \frac{e^{-t_n} e^{\Delta s_n} (1 - e^{-2\Delta s_n})}{1 - e^{-2t_n}} \langle \bar{\mathbf{x}}_0 \rangle, \\ \operatorname{Var}[\tilde{X}_{s_{n+1}} | \tilde{X}_{s_n}] &= 2 \sinh(t_{n+1}) \frac{\sinh(\Delta s_n)}{\sinh(t_n)} \\ &= (e^{t_{n+1}} - e^{-t_{n+1}}) \frac{e^{\Delta s_n} - e^{-\Delta s_n}}{e^{t_n} - e^{-t_n}} \\ &= \frac{e^{t_{n+1}} (1 - e^{-2t_{n+1}}) e^{\Delta s_n} (1 - e^{-2\Delta s_n})}{e^{t_n} (1 - e^{-2t_n})}. \end{aligned}$$

□

We summarize our discussion in the figures 8 and 9. The derivation of the stable diffusion algorithm (4.22) using the linear SDE (4.20) is more complicated than the standard method using the PDE and Bayes' formula. However, one possible advantage is that higher-order numerical schemes might be employed [19] to solve the SDE more accurately.

4.4 Approximative flow and loss function

Whether we want to solve the reverse dynamics (4.6) (score-matching) or to invert the forward process (4.22) (stable diffusion), the main difficulty relies on the estimation of the score $\nabla \ln \rho(x, t)$ or equivalently $\bar{\mathbf{x}}_0$ (4.3). Since ρ_0 is unknown, the explicit formula for $\bar{\mathbf{x}}_0$ (4.3) cannot be used. Instead, the usual approach [35] is to train a neural network (or any type of parametrized function), denoted by \mathbf{s}_θ , to approximate the score $\nabla \ln \rho$:

$$\mathbf{s}_\theta(x, t) \approx \nabla \ln \rho(x, t) \quad \text{for } 0 \leq t \leq T_*, x \in \mathbb{R}^d. \quad (4.25)$$

The parameters θ are then obtained by minimizing the mean-square error over the trajectories:

$$\ell[\theta] = \mathbb{E}_{\substack{t \sim U([0, T_*]) \\ X_t \sim \rho_t}} \left[\left| \mathbf{s}_\theta(X_t, t) - \nabla \ln \rho(X_t, t) \right|^2 \right], \quad (4.26)$$

The explicit expression for $\nabla \ln \rho$ (4.4) motivates the following ‘‘Ansatz’’ for \mathbf{s}_θ :

$$\mathbf{s}_\theta(x, t) = \frac{e^{-t} \bar{\mathbf{x}}_\theta(x, t) - x}{1 - e^{-2t}} \quad (4.27)$$

where now the neural network $\bar{\mathbf{x}}_\theta$ aims to approximate $\bar{\mathbf{x}}_0$. Then the loss (4.26) becomes

$$\ell[\theta] = \mathbb{E}_{\substack{t \sim U([0, T_*]) \\ X_t \sim \rho_t}} \left[c^2(t) (\bar{\mathbf{x}}_\theta(X_t, t) - \bar{\mathbf{x}}_0(X_t, t))^2 \right] \quad \text{with } c(t) = \frac{e^{-t}}{1 - e^{-2t}}. \quad (4.28)$$

Given that $\bar{\mathbf{x}}_0$ is already an expectation (4.2), we can use the bias-variance decomposition to rewrite the loss as:

$$\ell[\theta] = \mathbb{E}_{\substack{t \sim U([0, T_*]) \\ X_0 \sim \rho_0}} \left[c^2(t) (\bar{\mathbf{x}}_\theta(X_t, t) - X_0)^2 \right] - \mathbb{E}_{\substack{t \sim U([0, T_*]) \\ X_0 \sim \rho_0}} \text{Var} [c(t) \bar{\mathbf{x}}_0(X_t, t)], \quad (4.29)$$

where X_t is given by the explicit formula (2.12). Since the variance of $\bar{\mathbf{x}}_0$ is independent of θ , we can ignore it in the minimization and consider only the lefthand side (the *total loss*):

$$\ell_{total}[\theta] = \mathbb{E}_{\substack{t \sim U([0, T_*]) \\ X_0 \sim \rho_0}} \left[c^2(t) (\bar{\mathbf{x}}_\theta(X_t, t) - X_0)^2 \right]. \quad (4.30)$$

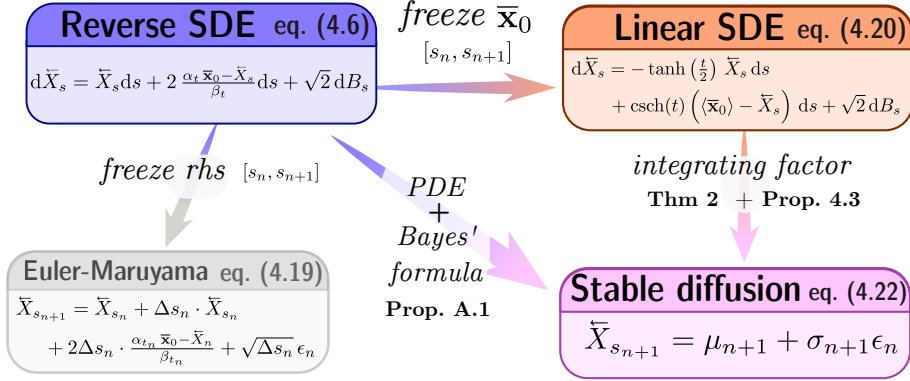


Figure 8: Derivation of the discrete algorithm used in stable diffusion from the reverse SDE (4.6). Assuming \bar{x}_0 constant over a time interval $[s_n, s_{n+1}]$, the reverse SDE (4.6) is integrable (4.12), leading to the discrete formula (4.22). Another way to derive the numerical scheme is to apply the Bayes' formula to the forward PDE (see Appendix A for details).

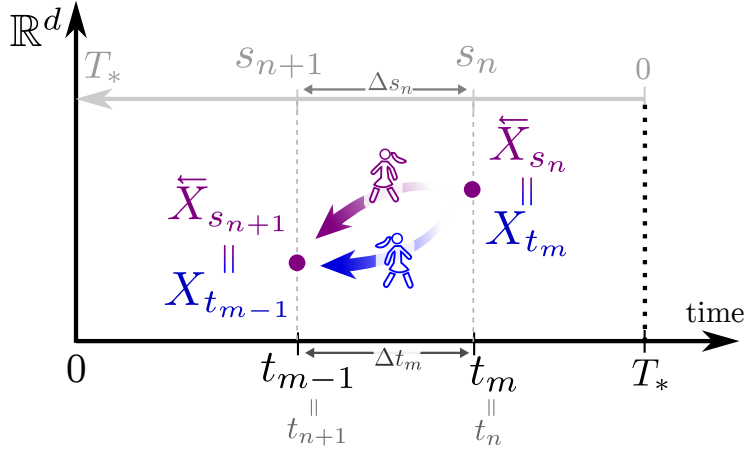


Figure 9: Two ways to derive the numerical scheme of the stable diffusion (4.22). First, as a forward discretization of the reverse dynamics (4.6) represented in magenta in the figure (see also figure 8). Second, as a *backward-in-time* discretization of the forward dynamics (2.11) represented in blue in the figure (see also Appendix A).

Notice that the loss ℓ_{total} is lower bounded by the variance term in (4.29), hence ℓ_{total} cannot converge to zero regardless of the neural network used for $\bar{\mathbf{x}}_\theta$.

Another modification proposed in [15] is to use the explicit solution of the forward process (2.12) to write X_0 as a function of X_t :

$$X_t = e^{-t}X_0 + \sqrt{1 - e^{-2t}}\varepsilon_0 \Rightarrow X_0 = e^tX_t - e^t\sqrt{1 - e^{-2t}}\varepsilon_0, \quad (4.31)$$

where $\varepsilon_0 \sim \mathcal{N}(0, \text{Id})$. Thus, we can use another Ansatz to predict X_0 :

$$\bar{\mathbf{x}}_\theta(X_t, t) = e^tX_t - e^t\sqrt{1 - e^{-2t}}\bar{\varepsilon}_\theta(X_t, t) \quad (4.32)$$

where now the neural network $\bar{\varepsilon}_\theta$ aims to predict the added noise ε_0 to the original sample. Plugging in the previous formula into the total loss ℓ_{total} 4.30 gives:

$$\ell_{total}[\theta] = \mathbb{E}_{\substack{t \sim U([0, T_*]) \\ X_0 \sim \rho_0 \\ \varepsilon_0 \sim \mathcal{N}(0, \text{Id})}} \left[\frac{1}{1 - e^{-2t}} (\bar{\varepsilon}_\theta(X_t, t) - \varepsilon_0)^2 \right], \quad (4.33)$$

where X_t is given by (4.31). Notice that the weight $1/(1 - e^{-2t})$ is singular as $t \rightarrow 0$. To avoid the singularity, the integral is replaced by a finite (Riemann) sum with a non-uniform discretization in time $0 = t_0 < \dots < t_{m_*} = T_*$:

$$\tilde{\ell}_{total}[\theta] = \mathbb{E}_{\substack{X_0 \sim \rho_0 \\ k \in [1, m_*]}} \left[(\bar{\varepsilon}_\theta(X_{t_k}, t_k) - \varepsilon_0)^2 \right], \quad (4.34)$$

where the discretization $\Delta t_k = t_{k+1} - t_k$ is smaller as t gets close to zero, hence more weight is given to the loss for t close to zero.

After minimization, the score $\mathbf{s}_\theta(x, t)$ is computed in the following three steps:

- i) Predict the noise level: $\tilde{\varepsilon} = \bar{\varepsilon}_\theta(x, t)$,
- ii) Deduce the expected origin: $\tilde{x}_0 = e^t x - e^t \sqrt{1 - e^{-2t}} \tilde{\varepsilon}$,
- iii) Reconstruct the score: $\mathbf{s}_\theta(x, t) = \frac{e^{-t} \tilde{x}_0 - x}{1 - e^{-2t}}$.

Notice that there is no need to reconstruct the score \mathbf{s}_θ if one resorts to the stable diffusion formulation (4.22).

4.5 Overfitting regime and kernel formulation

Whichever loss function we use (i.e. ℓ (4.26), ℓ_{total} (4.30), or $\tilde{\ell}_{total}$ (4.34)), the minimizer is explicitly given by $\bar{\mathbf{x}}_0$ (4.2) as the expected value is the unique minimizer of the mean square error. The parametric solution \mathbf{s}_θ can only approach the non-parametric solution $\bar{\mathbf{x}}_0$ and, in some sense, $\bar{\mathbf{x}}_0$ is the optimal limit of \mathbf{s}_θ as the neural network gets infinitely large.

However, the explicit formulation for $\bar{\mathbf{x}}_0$ (4.3) cannot be used as the density ρ_0 is unknown. The same problem occurs when estimating the different loss

functions previously introduced. In the absence of ρ_0 , the sampling $X_0 \sim \rho_0$ in the loss (4.34) is replaced in practice by a uniform sampling over the known samples $\{\mathbf{x}_i\}_{i=1}^N$. In other words, the empirical risk is used. However, in this specific case, one can compute $\bar{\mathbf{x}}_0$ explicitly, leading to a kernel formulation (note that similar formulations were found in [13] and [40]).

Proposition 4.4 *Suppose the initial distribution ρ_0 is uniform over the samples $\{\mathbf{x}_i\}_{i=1}^N$, i.e.,*

$$\rho_0(x) = \frac{1}{N} \sum_{i=1}^N \delta_{\mathbf{x}_i}(x), \quad (4.35)$$

where δ_x is the Dirac mass centered at x . Then the expected value $\bar{\mathbf{x}}_0$ (4.2) is explicit and given by the following kernel formulation:

$$\bar{\mathbf{x}}_0(x, t) = \sum_{i=1}^N \lambda_i(x, t) \mathbf{x}_i, \quad (4.36)$$

where $\{\lambda_i(x, t)\}_{i=1}^N$ is a convex combination given by

$$\lambda_i(x, t) = \frac{\rho(x, t | \mathbf{x}_i, 0)}{\sum_{j=1}^N \rho(x, t | \mathbf{x}_j, 0)} \quad (4.37)$$

with $\rho(\cdot, t | y, 0) \sim \mathcal{N}(e^{-t}y, \beta_t^2 Id)$ and $\beta_t^2 = 1 - e^{-2t}$.

Proof. Plugging in the expression of ρ_0 (4.35) into (4.3) and then using the fact that

$$\rho(x, t) = \int_{y \in \mathbb{R}^d} \rho(x, t | y, 0) \rho_0(y) dy \quad (4.38)$$

finishes the proof. \square

The weight $\lambda_i(x, t)$ (4.37) encodes the probability that $X_0 = \mathbf{x}_i$ given that $X_t = x$. An alternative handy expression of the vector $\boldsymbol{\lambda} = (\lambda_1, \dots, \lambda_N)$ is given by

$$\boldsymbol{\lambda}(x, t) = \text{Softmax} \left(-\frac{|x - e^{-t} \mathbf{x}_1|^2}{2\beta_t^2}, \dots, -\frac{|x - e^{-t} \mathbf{x}_N|^2}{2\beta_t^2} \right), \quad (4.39)$$

with Softmax representing the usual softmax function. Notice that as $t \gg 1$, the weights λ_i become uniform, i.e.,

$$\boldsymbol{\lambda}(x, t) \xrightarrow{t \rightarrow +\infty} \left(\frac{1}{N}, \dots, \frac{1}{N} \right), \quad (4.40)$$

leading $\bar{\mathbf{x}}_0$ (4.36) to become the mean of the samples $\{\mathbf{x}_i\}_{i=1}^N$. On the other hand, as $t \rightarrow 0$, the vector $\boldsymbol{\lambda}$ becomes (almost surely) a one-hot vector:

$$\boldsymbol{\lambda}(x, t) \xrightarrow{t \rightarrow 0} (0, \dots, 0, 1, 0, \dots, 0) \quad (4.41)$$

where the value 1 indicates the closest sample \mathbf{x}_i to x . We can further formalize this observation by introducing the Voronoi tessellation $\{\mathcal{C}_i\}_{i=1}^N$ associated with the samples $\{\mathbf{x}_i\}_{i=1}^N$:

$$\mathcal{C}_i = \{x \in \mathbb{R}^d \mid |x - \mathbf{x}_i| = \min(|x - \mathbf{x}_1|, \dots, |x - \mathbf{x}_N|)\}. \quad (4.42)$$

Then as $t \rightarrow 0$, the expected value $\bar{\mathbf{x}}_0$ becomes constant on the (interior of the) Voronoi cells \mathcal{C}_i :

$$\bar{\mathbf{x}}_0(x, t) \xrightarrow{t \rightarrow 0} \mathbf{x}_i \quad \text{for } x \in \overset{\circ}{\mathcal{C}}_i. \quad (4.43)$$

Moreover, the reverse diffusion becomes a stiff relaxation as $t \rightarrow 0$ (4.8). Thus, for $\bar{X}_s \in \overset{\circ}{\mathcal{C}}_i$,

$$d\bar{X}_s \stackrel{t \rightarrow 0}{\approx} \frac{1}{t} (\mathbf{x}_i - \bar{X}_s) ds + \mathcal{O}(1) ds + \sqrt{2} dB_s. \quad (4.44)$$

As $t \rightarrow 0$, the process \bar{X}_s becomes more attracted to \mathbf{x}_i and is more likely to stay inside the Voronoi cell $\overset{\circ}{\mathcal{C}}_i$.

The previous observations are rather informal. The Corollary 3.3 provides a more clear statement: as the support of ρ_0 consists of the discrete sample points, the reverse process will eventually converge to one of the original sample (see figure 10 for an illustration):

$$\bar{X}_s \xrightarrow{s \rightarrow T^*} \mathbf{x}_i. \quad (4.45)$$

Thus, solving the minimization problem *exactly* is counter-productive: the generative flow does nothing but sample from the original samples. Hence, there is an inherent risk of overfitting regime when applying the reverse diffusion dynamics since there is no inherent regularization unless penalization terms are added.

5 Conclusion

In this manuscript, we have shown that reverse diffusion, if executed exactly, does not regularize the original sample distribution ρ_0 . Indeed, by perfectly reconstructing the forward process, the resulting generated distribution q_{T^*} (2.7) has its support entirely contained within the support of ρ_0 (corollary 3.3). In other words, generated samples cannot be “out-of-the-sample.” Consequently, for a finite number of samples, exact reverse diffusion will merely reproduce one of the original samples.

In practice, score-matching or stable diffusion (4.22)-(4.24) does not precisely follow the reverse diffusion process because it introduces a minimization problem (4.26) that is not solved exactly. However, it is relatively straightforward to derive an explicit formula (e.g., using the kernel formulation in Proposition (4.35)) for the minimization problem. That said, this computation becomes impractical when the number of original samples N is large. This leads to an apparent paradox: when the minimization problem is solved too accurately, the generative method closely approximates the reverse diffusion process, and

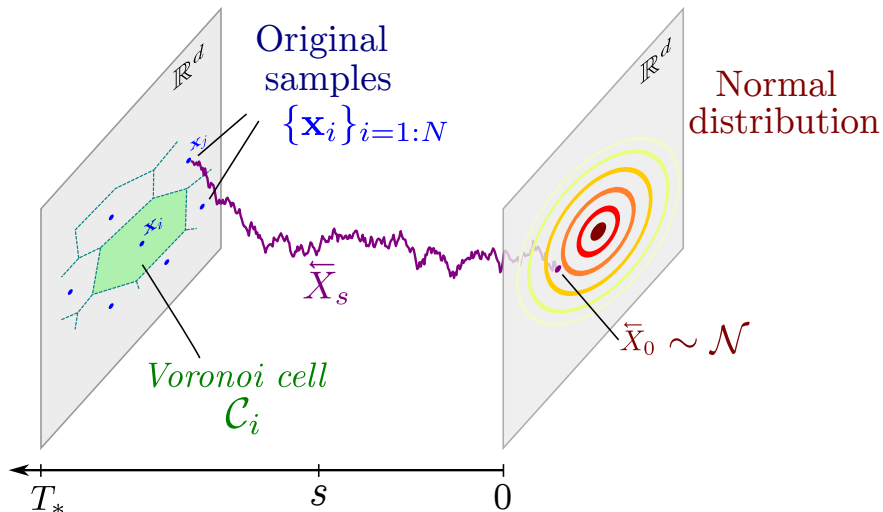


Figure 10: Starting from a normal distribution (right), the reverse process \tilde{X}_s becomes trapped into a Voronoi cell \mathcal{C}_i (4.42) as $t \rightarrow 0$ and eventually converges to a sample \mathbf{x}_i as stated by Corollary 3.3.

thus no new samples are generated (see, e.g., [27] for a condition under which no generalization occurs). Paradoxically, the minimization problem must be “imperfect” for the generative method to produce novel samples.

A simple extension of our work would involve demonstrating that (discrete) stable diffusion, in the overfitting regime, indeed converges to the original samples. While we have established this result for the continuous reverse diffusion formulation as a consequence of Corollary 3.3, it remains to be rigorously proven for the discrete algorithm.

More broadly, our results raise the question of when generalization occurs when applying reverse diffusion. Reverse diffusion by itself does not “generalize.” A simpler way to express this is to say that “*everything is in the UNet*”. Indeed, for image generation, a UNet architecture is used to estimate the expected origin $\bar{\mathbf{x}}_0$ (4.2) (or, equivalently, the expected noise ϵ_0). Without it, the overall machinery of the reverse diffusion process would not work. Thus, one has to study the interplay between the reverse dynamics diffusion and the UNet approximation. The flow introduces a mixing property that combines different images intelligently [17] without assuming that relevant images lie on a low-dimensional manifold (as in the variational auto-encoder approach). Interestingly, the neural approximation of the score is “imperfect” enough to generate new data points. Using the kernel formulation in the overfitting regime, one can identify when the practical flow starts to deviate from the exact flow, thereby characterizing the “good error” necessary for generating new samples.

A Formula for stable diffusion

Denote by ρ the law of the forward process (2.11). Fix a partition $0 = t_0 < t_1 < \dots < t_m < \dots < T_*$ with $\Delta t_m = t_m - t_{m-1}$, and set $X_m = X_{t_m}$. We define $\rho(X_m | X_{m-1})$ to be the law of ρ at time t_m knowing X_{m-1} . Using our pairwise distribution (2.23), this is equivalent to

$$\rho(X_m = y | X_{m-1} = x) = \rho(y, t_m | x, t_{m-1}). \quad (\text{A.1})$$

Our goal is to reverse the equation (A.1) and express the probability of the past position X_{m-1} knowing the future X_m . The trick is once again to assume that we know the starting position x_0 .

Proposition A.1

$$\rho(X_{m-1} | X_m, x_0) \sim \mathcal{N}(\bar{\mu}_{m-1}, \bar{\sigma}_{m-1}^2 \text{Id}) \quad (\text{A.2})$$

with

$$\bar{\mu}_{m-1} = \frac{e^{-\Delta t_m} (1 - e^{-2t_{m-1}})}{1 - e^{-2t_m}} X_m + \frac{e^{-t_{m-1}} (1 - e^{-2\Delta t_m})}{1 - e^{-2t_m}} x_0, \quad (\text{A.3})$$

$$\bar{\sigma}_{m-1}^2 = \frac{(1 - e^{-2\Delta t_m})(1 - e^{-2t_{m-1}})}{1 - e^{-2t_m}}. \quad (\text{A.4})$$

Proof. We start by invoking the Bayes' formula:

$$\rho(X_{m-1} | X_m, x_0) = \frac{\rho(X_m | X_{m-1}, x_0) \cdot \rho(X_{m-1} | x_0)}{\rho(X_m | x_0)} \quad (\text{A.5})$$

$$= c \cdot \rho(X_m | X_{m-1}) \cdot \rho(X_{m-1} | x_0), \quad (\text{A.6})$$

using the Markov property and the fact that the numerator is constant in X_{m-1} . Notice that the notation is somewhat confusing here since $\rho(X_m | X_{m-1})$ has to be seen as a function of X_{m-1} and not X_m . Hence,

$$\rho(X_m | X_{m-1}) = c \exp\left(-\frac{|X_m - e^{-\Delta t_m} X_{m-1}|^2}{2(1 - e^{-2\Delta t_m})}\right) = c \exp\left(-\frac{|e^{\Delta t_m} X_m - X_{m-1}|^2}{2(e^{2\Delta t_m} - 1)}\right).$$

To conclude, we only need to apply Lemma A.2 with

$$\rho(X_m | X_{m-1}) \sim \mathcal{N}(e^{\Delta t_m} X_m, (e^{2\Delta t_m} - 1)\text{Id}) \quad (\text{A.7})$$

$$\rho(X_{m-1} | x_0) \sim \mathcal{N}(e^{-t_{m-1}} x_0, (1 - e^{-2t_{m-1}})\text{Id}), \quad (\text{A.8})$$

leading to $\rho(X_{m-1} | X_m, x_0) \sim \mathcal{N}(\bar{\mu}, \bar{\sigma}^2 \text{Id})$ with

$$\bar{\mu} = \frac{(1 - e^{-2t_{m-1}})e^{\Delta t_m} X_m}{(e^{2\Delta t_m} - 1) + (1 - e^{-2t_{m-1}})} + \frac{(e^{2\Delta t_m} - 1)e^{-t_{m-1}} x_0}{(e^{2\Delta t_m} - 1) + (1 - e^{-2t_{m-1}})}.$$

We recognize the formula for $\bar{\mu}_{m-1}$ (A.3). Similarly, we have

$$\bar{\sigma}^2 = \frac{(e^{2\Delta t_m} - 1) \cdot (1 - e^{-2t_{m-1}})}{(e^{2\Delta t_m} - 1) + (1 - e^{-2t_{m-1}})} = \frac{(e^{2\Delta t_m} - 1) \cdot (1 - e^{-2t_{m-1}})}{e^{2\Delta t_m} (1 - e^{-2t_m})}.$$

□

Lemma A.2 Suppose $f \sim \mathcal{N}(\mu_1, \sigma_1^2 Id)$ and $g \sim \mathcal{N}(\mu_2, \sigma_2^2 Id)$. Then

$$h(z) = cf(z)g(z) \sim \mathcal{N}(\bar{\mu}, \bar{\sigma}^2 Id), \quad (\text{A.9})$$

where $c > 0$ is a normalizing constant with

$$\bar{\mu} = \frac{\sigma_2^2 \mu_1 + \sigma_1^2 \mu_2}{\sigma_1^2 + \sigma_2^2} \quad \text{and} \quad \bar{\sigma}^2 = \frac{\sigma_1^2 \sigma_2^2}{\sigma_1^2 + \sigma_2^2}. \quad (\text{A.10})$$

Proof. We multiply the two Gaussian distributions:

$$\begin{aligned} f(z) \cdot g(z) &= c \exp\left(-\frac{|z - \mu_1|^2}{2\sigma_1^2} - \frac{|z - \mu_2|^2}{2\sigma_2^2}\right) \\ &= c \exp\left(-\frac{\sigma_2^2 |z - \mu_1|^2 + \sigma_1^2 |z - \mu_2|^2}{2\sigma_1^2 \sigma_2^2}\right) =: c \exp\left(-\frac{A}{2\sigma_1^2 \sigma_2^2}\right). \end{aligned}$$

Now we complete the square:

$$\begin{aligned} A &= (\sigma_1^2 + \sigma_2^2)|z|^2 - 2\sigma_2^2 \langle \mu_1, z \rangle - 2\sigma_1^2 \langle \mu_2, z \rangle + \sigma_1^2 \mu_1^2 + \sigma_2^2 \mu_2^2 \\ &= s^2 |z|^2 - 2s^2 \langle \bar{\mu}, z \rangle + \sigma_1^2 \mu_1^2 + \sigma_2^2 \mu_2^2 \end{aligned}$$

with $s^2 = \sigma_1^2 + \sigma_2^2$ and $\bar{\mu}$ given by (A.10). Thus,

$$A = s^2 |z - \bar{\mu}|^2 - s^2 |\bar{\mu}|^2 + \sigma_1^2 \mu_1^2 + \sigma_2^2 \mu_2^2.$$

We deduce that

$$f(z) \cdot g(z) = \tilde{c} \exp\left(-\frac{s^2 |z - \bar{\mu}|^2}{2\sigma_1^2 \sigma_2^2}\right) = \tilde{c} \exp\left(-\frac{|z - \bar{\mu}|^2}{2\bar{\sigma}^2}\right),$$

with $\bar{\sigma}^2$ given by (A.10). □

References

- [1] Brian DO Anderson. Reverse-time diffusion equation models. *Stochastic Processes and their Applications*, 12(3):313–326, 1982.
- [2] Dominique Bakry, Ivan Gentil, Michel Ledoux, et al. *Analysis and geometry of Markov diffusion operators*, volume 103. Springer, 2014.
- [3] Dmitry Baranchuk, Andrey Voynov, Ivan Rubachev, Valentin Khruikov, and Artem Babenko. Label-efficient semantic segmentation with diffusion models. In *International Conference on Learning Representations*, 2022.
- [4] Hongrui Chen, Holden Lee, and Jianfeng Lu. Improved analysis of score-based generative modeling: User-friendly bounds under minimal smoothness assumptions. In *International Conference on Machine Learning*, pages 4735–4763. PMLR, 2023.

- [5] Sitan Chen, Sinho Chewi, Jerry Li, Yuanzhi Li, Adil Salim, and Anru Zhang. Sampling is as easy as learning the score: theory for diffusion models with minimal data assumptions. In *The Eleventh International Conference on Learning Representations*, 2023.
- [6] Valentin De Bortoli, James Thornton, Jeremy Heng, and Arnaud Doucet. Diffusion schrödinger bridge with applications to score-based generative modeling. *Advances in Neural Information Processing Systems*, 34:17695–17709, 2021.
- [7] Pierre Degond and Sylvie Mas-Gallic. The weighted particle method for convection-diffusion equations. i. the case of an isotropic viscosity. *Mathematics of computation*, 53(188):485–507, 1989.
- [8] Prafulla Dhariwal and Alexander Nichol. Diffusion models beat gans on image synthesis. *Advances in neural information processing systems*, 34:8780–8794, 2021.
- [9] Sander Dieleman. Perspectives on diffusion. <https://sander.ai/2023/07/20/perspectives.html>, 2023.
- [10] Lawrence C Evans. *An introduction to stochastic differential equations*, volume 82. American Mathematical Soc., 2012.
- [11] Lawrence C Evans. *Partial differential equations*, volume 19. American Mathematical Society, 2022.
- [12] Shansan Gong, Mukai Li, Jiangtao Feng, Zhiyong Wu, and LingPeng Kong. Diffuseq: Sequence to sequence text generation with diffusion models. *arXiv preprint arXiv:2210.08933*, 2022.
- [13] Xiangming Gu, Chao Du, Tianyu Pang, Chongxuan Li, Min Lin, and Ye Wang. On memorization in diffusion models. *arXiv preprint arXiv:2310.02664*, 2023.
- [14] Ulrich G Haussmann and Etienne Pardoux. Time reversal of diffusions. *The Annals of Probability*, pages 1188–1205, 1986.
- [15] Jonathan Ho, Ajay Jain, and Pieter Abbeel. Denoising diffusion probabilistic models. *Advances in neural information processing systems*, 33:6840–6851, 2020.
- [16] Jonathan Ho, Tim Salimans, Alexey Gritsenko, William Chan, Mohammad Norouzi, and David J Fleet. Video diffusion models. *Advances in Neural Information Processing Systems*, 35:8633–8646, 2022.
- [17] Zahra Kadkhodaie, Florentin Guth, Eero P Simoncelli, and Stéphane Mallat. Generalization in diffusion models arises from geometry-adaptive harmonic representation. *arXiv preprint arXiv:2310.02557*, 2023.

- [18] Tero Karras, Miika Aittala, Timo Aila, and Samuli Laine. Elucidating the design space of diffusion-based generative models. *Advances in neural information processing systems*, 35:26565–26577, 2022.
- [19] Peter E Kloeden, Eckhard Platen, Peter E Kloeden, and Eckhard Platen. *Stochastic differential equations*. Springer, 1992.
- [20] Zhifeng Kong, Wei Ping, Jiaji Huang, Kexin Zhao, and Bryan Catanzaro. Diffwave: A versatile diffusion model for audio synthesis. In *International Conference on Learning Representations*, 2021.
- [21] Sixu Li, Shi Chen, and Qin Li. A good score does not lead to a good generative model. *arXiv preprint arXiv:2401.04856*, 2024.
- [22] Xiang Li, John Thickstun, Ishaan Gulrajani, Percy S Liang, and Tatsunori B Hashimoto. Diffusion-lm improves controllable text generation. *Advances in Neural Information Processing Systems*, 35:4328–4343, 2022.
- [23] Nikiforos Mimikos-Stamatopoulos, Benjamin J Zhang, and Markos A Katsoulakis. Score-based generative models are provably robust: an uncertainty quantification perspective. *arXiv preprint arXiv:2405.15754*, 2024.
- [24] Alexander Quinn Nichol and Prafulla Dhariwal. Improved denoising diffusion probabilistic models. In *International conference on machine learning*, pages 8162–8171. PMLR, 2021.
- [25] Bernt Oksendal. *Stochastic differential equations: an introduction with applications*. Springer Science & Business Media, 2013.
- [26] Etienne Pardoux, Aurel Răşcanu, Etienne Pardoux, and Aurel Răşcanu. *Stochastic differential equations*. Springer, 2014.
- [27] Jakiw Pidstrigach. Score-based generative models detect manifolds. *Advances in Neural Information Processing Systems*, 35:35852–35865, 2022.
- [28] Ben Poole, Ajay Jain, Jonathan T. Barron, and Ben Mildenhall. Dreamfusion: Text-to-3d using 2d diffusion. In *The Eleventh International Conference on Learning Representations*, 2023.
- [29] Vadim Popov, Ivan Vovk, Vladimir Gogoryan, Tasnima Sadekova, and Mikhail Kudinov. Grad-tts: A diffusion probabilistic model for text-to-speech. In Marina Meila and Tong Zhang, editors, *Proceedings of the 38th International Conference on Machine Learning*, volume 139 of *Proceedings of Machine Learning Research*, pages 8599–8608. PMLR, 18–24 Jul 2021.
- [30] Chitwan Saharia, William Chan, Huiwen Chang, Chris Lee, Jonathan Ho, Tim Salimans, David Fleet, and Mohammad Norouzi. Palette: Image-to-image diffusion models. In *ACM SIGGRAPH 2022 conference proceedings*, pages 1–10, 2022.

- [31] Bernard W Silverman. *Density estimation for statistics and data analysis*. Routledge, 2018.
- [32] Jascha Sohl-Dickstein, Eric Weiss, Niru Maheswaranathan, and Surya Ganguli. Deep unsupervised learning using nonequilibrium thermodynamics. In *International conference on machine learning*, pages 2256–2265. PMLR, 2015.
- [33] Gowthami Somepalli, Vasu Singla, Micah Goldblum, Jonas Geiping, and Tom Goldstein. Diffusion art or digital forgery? investigating data replication in diffusion models. In *Proceedings of the IEEE/CVF Conference on Computer Vision and Pattern Recognition (CVPR)*, pages 6048–6058, June 2023.
- [34] Yang Song, Conor Durkan, Iain Murray, and Stefano Ermon. Maximum likelihood training of score-based diffusion models. *Advances in neural information processing systems*, 34:1415–1428, 2021.
- [35] Yang Song and Stefano Ermon. Generative modeling by estimating gradients of the data distribution. *Advances in neural information processing systems*, 32, 2019.
- [36] Yang Song and Stefano Ermon. Improved techniques for training score-based generative models. *Advances in neural information processing systems*, 33:12438–12448, 2020.
- [37] Yang Song, Jascha Sohl-Dickstein, Diederik P Kingma, Abhishek Kumar, Stefano Ermon, and Ben Poole. Score-based generative modeling through stochastic differential equations. *arXiv preprint arXiv:2011.13456*, 2020.
- [38] Alexandre Thiéry. Denoising diffusion probabilistic models (ddpm). <https://alexthiery.github.io/notes/DDPM/DDPM.html>, 2023.
- [39] Lilian Weng. What are diffusion models? <https://lilianweng.github.io/posts/2021-07-11-diffusion-models/>, Jul 2021.
- [40] Mingyang Yi, Jiacheng Sun, and Zhenguo Li. On the generalization of diffusion model. *arXiv preprint arXiv:2305.14712*, 2023.
- [41] Benjamin J Zhang and Markos A Katsoulakis. A mean-field games laboratory for generative modeling. *arXiv preprint arXiv:2304.13534*, 2023.